Liquid Crystals
Publication details, including instructions for authors and subscription information:
http://www.informaworld.com/smpp/title~content=t713926090

Time resolved X-ray diffraction studies of electric field induced layer motion in a chevron geometry smectic A liquid crystal device

A. S. Morse; H. F. Gleeson; S. Cummings

Online publication date: 29 June 2010

To cite this Article Morse, A. S. , Gleeson, H. F. and Cummings, S.(1997) 'Time resolved X-ray diffraction studies of electric field induced layer motion in a chevron geometry smectic A liquid crystal device', Liquid Crystals, 23: 5, 717 — 722
To link to this Article: DOI: 10.1080/026782997207993
URL: http://dx.doi.org/10.1080/026782997207993

LIQUID CRYSTALS, 1997, VOL. 23, NO. 5, 717–722

Time resolved X-ray diffraction studies of electric field induced layer motion in a chevron geometry smectic A liquid crystal device

by A. S. MORSE, H. F. GLEESON* and S. CUMMINGS
The Department of Physics and Astronomy, Manchester University, Manchester M13 9PL, United Kingdom

(*Received 10 March 1997; accepted 18 June 1997*)

Small angle time-resolved X-ray diffraction was used to monitor the behaviour of the smectic layers during the electric field induced planar to homeotropic transition in a smectic A cell possessing a chevron layer geometry. The liquid crystal material used was S3, from Merck Ltd, and was sandwiched in a 15 μm parallel plate device. The main features of the transition are the cooperative rotation of layers and the creation of an asymmetric chevron structure during the early stages of switching. The time scale for the planar-to-homeotropic transition in the device is approximately 5 s, at a temperature of 3°C below the nematic-to-smectic A phase transition and for an applied electric field of 2 V μm^{-1} (rms).

1. Introduction

X-ray diffraction has been used extensively to show the arrangement of smectic layers in display-type cells. The chevron structure adopted by the layers within ferroelectric liquid crystal (FLC) devices was first elucidated by X-ray measurements [1]; the chevron structure forms in these systems as a consequence of layer thinning due to an increasing tilt cone angle on cooling [2]. There have been only a few reports of a chevron structure in the smectic A phase [3–6]. The smectic A chevron structure forms in those materials whose layer spacing decreases on cooling due to conformational changes.

If an electric field is applied across a planar smectic A cell of material of positive dielectric anisotropy, this anisotropy will couple with the field and rotate the average direction of the molecules, the director, until it is aligned homeotropically [7]. There have until now been no studies of the electric field induced 'planar' to homeotropic transition in smectic A cells known to have a chevron structure. Furthermore there have hitherto been no time-resolved X-ray studies of this transition, even in bookshelf devices. Only the behaviour of the director has been monitored, using the technique of polarizing microscopy [8–11]. This means that the behaviour of the smectic layers during switching has not been observed directly. Time-resolved X-ray diffraction studies of the layer behaviour during low electric field director reorientation have recently been reported for the surface stabilized ferroelectric liquid crystal device [12]. In this paper we use the same technique to study the electric field induced planar-to-homeotropic transition in a smectic A cell possessing a chevron structure.

*Author for correspondence.

2. Experimental

The 15-μm-thick smectic A sample (S3 from Merck Ltd) was prepared in a parallel-plate cell with thin ITO electrodes, in a method similar to that described in a previous paper [6]. S3 exhibits a smectic A to nematic phase transition at 54·5°C and becomes isotropic at 59°C. The cell had antiparallel rubbed PVA alignment layers. The X-ray apparatus and heating apparatus were also similar to those described previously [12, 13]. The sample temperature was maintained at 51·5°C throughout the experiment. This temperature (3°C below the nematic-to-smectic A transition temperature) was chosen, in conjunction with the applied electric field (30 Vrms, 1 kHz), to give a switching time large enough to be recorded using the minimum acceptable data collection time frame size (0·5 s). The 10–90% switching time of ~5 s was measured optically in a subsidiary experiment (not reported in detail here) using a polarizing microscope and photodiode arrangement. The beam size at the sample was 1 mm × 1 mm. The device was rocked about a vertical axis, with peaks in the rocking curve occurring when the layers were oriented to the Bragg condition. The angular precision was 0·072°, although for practical reasons the rocking angle step size was chosen to be 2°.

The data relating to layer motion after field application were recorded as follows. The cell was rotated to

0267–8292/97 $12·00

$-20°$; the switching electric field was then applied to the sample, in synchronization with data collection from the area detector. Synchronization was controlled by a time frame generator (TFG) which triggered a function generator to output the chosen voltage to the sample, thus switching the director. Data were subsequently collected in 0·5 s time frames over a 10 s period (figure 1).

The sample was thermally realigned after (nonreversible) switching to restore it to the planar orientation; the cell was then rocked to $-18°$ and the switching experiment repeated. This process was continued at 2° intervals until the cell sat at a rocking angle of $+20°$. Rocking curves were then assembled for each time frame during switching. The use of an area detector allowed measurement of the Bragg angle throughout the experiments.

3. Results and discussion

There were no resolvable changes in the Bragg angle throughout the experiment. This implies that the layer spacing remains constant to within $\pm 0{\cdot}1$ Å during switching. Figure 2 shows the rocking curves obtained at each 0·5 s interval. Normalization, correction and integration procedures were similar to those described in a previous paper [6]. In this case, the relative error in integrated diffraction intensity varies from 5% for the strongest peak, to 29% for the weakest diffraction. The lines drawn in figure 2 are simply interpolations between data points and are intended as a guide to the eye. The small number of data points rendered meaningful curve fits impossible.

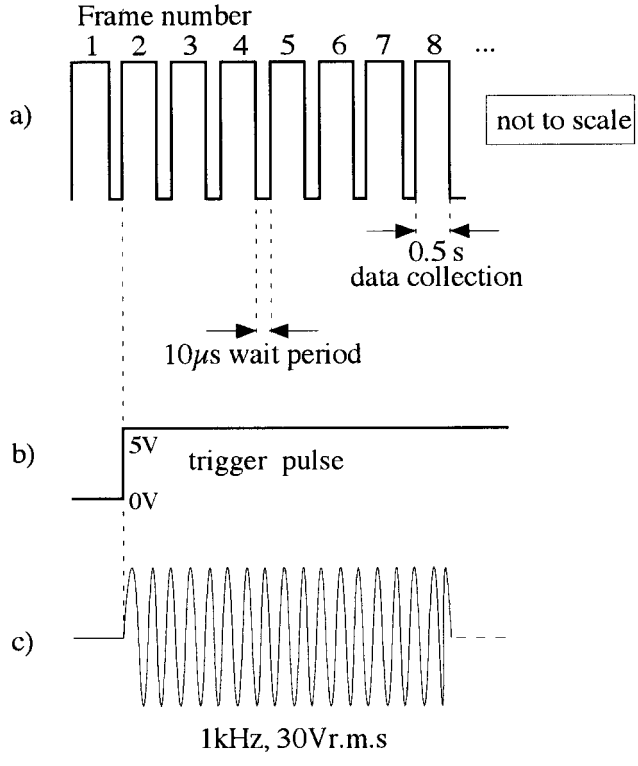

Figure 1. Experimental settings. (*a*) Data collection time frames; (*b*) trigger pulse to generator; (*c*) synchronized switching waveform to cell.

The 0 s curve shows the presence of a chevron structure in the unperturbed cell, the chevron angle being $\sim 5°$, which is approximately the same as the chevron angle measured (at the same temperature) for a 50 μm cell in a previous experiment [6]. Peaks A and B correspond to diffraction from each arm of the chevron structure. The difference in peak heights at the start of the experiment probably occurs because the integrated diffraction spot intensity is very sensitive to rocking angle and the (large) 2° rocking steps are insufficient to resolve the fine structure, though the possibility of the initial chevron structure being asymmetric cannot be ruled out. In the interests of clarity, in this discussion the initial structure shall be considered to be a symmetric chevron structure, although the proposed switching mechanisms would equally apply to an initially asymmetric chevron structure as might be expected to occur in an antiparallel rubbed low pretilt ($\sim 0{\cdot}5°$) device as studied here [14].

The persistence of diffraction peaks after electric field application indicates that the layers remain intact to some extent during switching. The angular shifts in peak position indicate that the two arms of the chevron structure rotate in opposite directions during switching, each towards its nearest cell wall (figure 3). This is expected since it means that the molecules swing around the easiest (more energetically favourable) path. Such motion of the chevron arms is only possible if, either the layers fracture at the chevron interface, or an asymmetric chevron forms; the possibilities are illustrated in figure 3 and discussed later. The layers marked A and B are those corresponding to diffraction peaks A and B in figure 2.

The angular rotation of the chevron arms is quantified in figure 4, where the angular position of each peak centre is plotted against time. The angular peak positions are plotted relative to the initial peak positions (designated 0°), and to make a comparison easier, the relative angular motion of peak B is shown as negative relative to that of peak A. The centre of peak A moves by about 5° in the first 2 s and stays at this angle. Within the same time, the centre of peak B moves by about 3° and continues moving slowly, even towards the end of the experiment, ~ 9 s after field application. The slower rotation rate of layers B with respect to layers A could be attributed to the formation of an asymmetric chevron structure early during switching (as proposed in figure 3), before layer disruption dominates the process. The initial chevron structure and the hypothesized asymmetric chevron structure are shown, to scale, in figure 5; the chevron structure probably becomes asymmetric due to

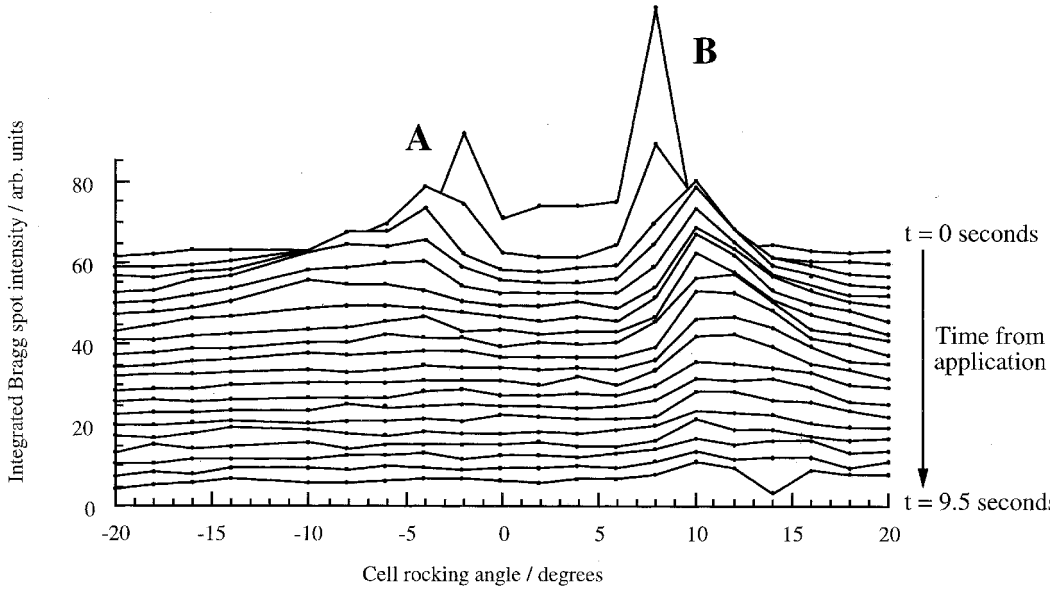

Figure 2. Assembled rocking curves. The integrated intensity of the diffraction spot (normalized) is plotted as a function of cell angle. Rocking curves are shown for each of the 0·5 s data collection frames. Lines connecting data points are included solely as a visual aid and do not represent a fit of any kind.

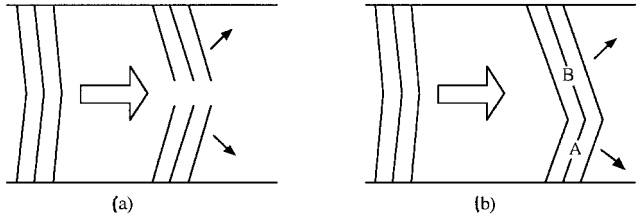

Figure 3. Possible rotations of the chevron arms during smectic A switching; the angles are exaggerated. Case (*a*) shows layer fracture; case (*b*) shows formation of an asymmetric chevron structure.

the combination of antiparallel surface alignment rubbing and pretilt (~0·5°) as shown in figure 6. The director in the initial chevron structure opposes the pretilt direction at both surfaces, thus introducing strain at the surface regions. When layers A begin to rotate, this strain decreases and the rotation is thus aided by the presence of pretilt; for layers B however, the strain increases and rotation is hindered. In this way the speed of layer rotation will differ between layers A and B, and an asymmetric chevron structure forms.

Figure 2 shows that both peaks become more diffuse during switching, although peak A spreads out much more quickly than peak B. The diffuse peaks correspond to a spread of layering directions, which probably arises due to structural fragmentation (the appearance of a multidomain structure). The domains (to be precise the layers within them) can rotate at slightly different speeds; as time progresses an angular distribution of layers thus results. This statement is corroborated by the fact that for each peak the outer edge becomes more diffuse than the inner edge, implying the existence of a minimum rotation rate. Although the majority of the layers, represented by the peak centres, move through ~3° or ~5°, some of the faster moving layers can move through much larger angles in the same time (up to ~15°). Differences in the rates of layer rotation may be due to

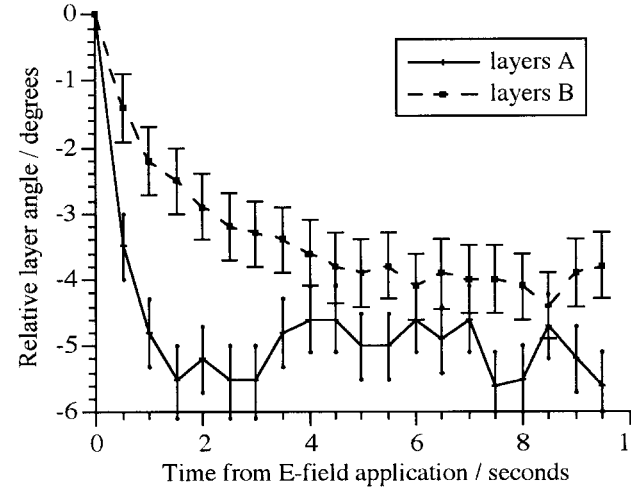

Figure 4. Angular rotation of the chevron arms during smectic A switching. Lines connecting data points are included solely as a visual aid and do not represent a fit of any kind.

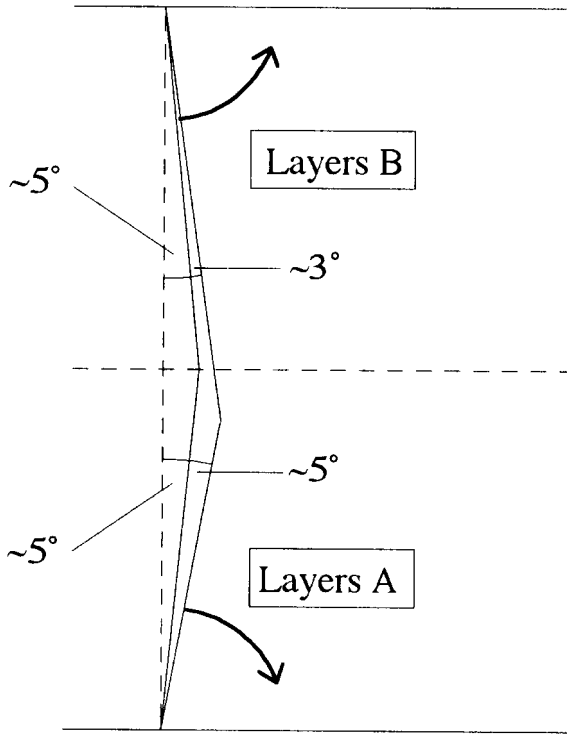

Figure 5. Scaled schematic diagram showing how an asymmetric chevron structure might form during switching. The angles marked correspond to the position of most of the layers after approximately 2 s.

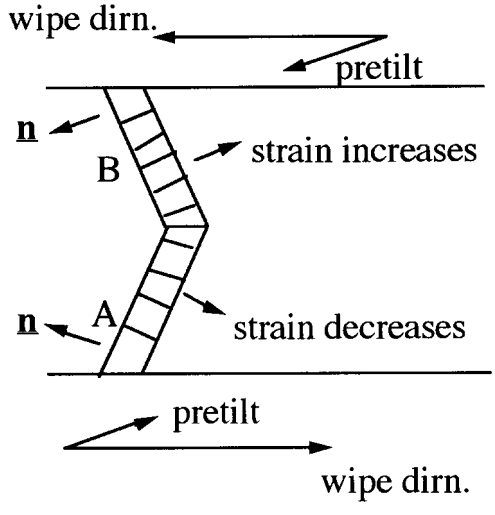

Figure 6. The effect of antiparallel alignment rubbing on the smectic A switching process. The angles are exaggerated for clarity.

a number of factors, e.g. domain size, proximity to alignment surfaces and proximity to the chevron apex.

The peaks (figure 2) also become less intense during switching. The spread in layer direction due to a rotating multidomain structure would itself lower the maximum

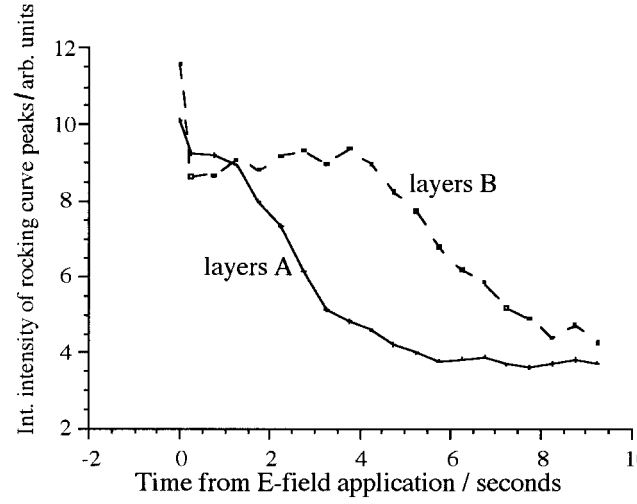

Figure 7. The total integrated intensity of each rocking curve peak against time from field application. Lines connecting data points are included solely as a visual aid and do not represent a fit of any kind.

peak intensity, but for each diffuse peak the overall diffracted intensity (the integrated intensity for all rocking angles under the peak) would remain constant. Figure 7 shows a plot of the integrated intensity of each peak against time from field application. Clearly the integrated intensity does not remain constant for the entire switching period, indicating that the spread in layer directions from one domain to the next is not the only reason for the decreasing maximum peak intensities in figure 2. The other possible reasons for the decrease in peak intensity are:

(i) Increased mosaicity (alignment spread) in the plane of the cell face during switching. Such an effect could possibly arise as a result of domains jostling each other during switching. The effect would have manifested itself, however, as an arcing of the diffraction spot on the detector; this was not seen.

(ii) Rapid rotation of the layers to the homeotropic state. This effect certainly occurs in the sample and is discussed more quantitatively below. The homeotropically oriented layers do not contribute to the Bragg scattering in the geometry examined here, and therefore result in a reduction in the intensity of the peaks.

(iii) Layer disruption. This seems likely, since it is not possible for all the domains to rotate cooperatively whilst maintaining a fixed layer structure. The driving force for the disruption is of course the electric torque on the molecules, so they would however rotate cooperatively and disruption would thus consist of the formation of

nematic-like regions. Layer disruption also occurs within domain walls, so that as the number of domains gets very large the diffraction peak intensity will fall accordingly.

Figure 7 also indicates for how long the layers A and B persist. The 90→10% decay time was calculated as ~2 s for layers A and ~6 s for layers B. The geometry of the experiment did not allow the final, switched layer structure of the system to be observed.

The proposal of an asymmetric chevron explains the difference in rotation rates of the layers A and B, and why the intensity of the diffuse peak B is larger than that of the diffuse peak A during switching (figure 2). A problem, however, is that as drawn in figure 5 this would necessitate an *increase* in the overall diffracted intensity from layers B during the initial stages of switching. Figure 7 shows a slight *decrease* in this intensity. The discrepancy is explained by the fact that some regions of the cell have undergone layer rotation to the homeotropic state very early in the switching process.

Optical studies of the switching process showed that switching began in the vicinity of cell defects and propagated more rapidly in a direction parallel to the layers than perpendicular to them. Similar behaviour has been reported by Jákli and Saupe [11]. The reason for this behaviour is that once one end of a layer begins to turn, the rest of the layer tries to remain intact and rotate with it. A study of photomicrographs of the switching in this device shows that approximately 25%, 50% and 90% of the sample area is homeotropic ~1 s, 2 s and 3 s after application of the field. Taking this into account, it is clear that the relative proportion of layers B does in fact increase during the switching process, as would be expected in the proposed switching mechanism.

A summary of the observations and proposed switching model is given below:

(1) The cell initially has a chevron structure, with a chevron angle of ~5°.
(2) On electric field application, the layers begin rotating cooperatively, introducing stress throughout the cell, which is relieved by the creation of a multidomain structure.
(3) The layers in each arm of the chevron rotate towards the adjacent cell wall.
(4) Switching begins near cell defects. Once one end of a group of layers rotates, the rotation will propagate along the layers. This happens in preference to cooperative rotation with neighbouring domains.
(5) Pretilt and antiparallel rubbing lead to the formation of a slightly asymmetric chevron structure.
(6) Layer rotation within each domain occurs at different rates.
(7) After a few seconds the asymmetric chevron structure breaks up. This is probably due to the large increase in elastic forces at the chevron apex, caused by the larger chevron angle. Previous studies of smectic A layer arrangements [6] have shown the existence of critical chevron angles above which these structures become energetically unfavourable.
(8) The chevron break-up introduces more domains and also, possibly nematic-like regions.
(9) The chevron arms fracture. The long arm of the asymmetric chevron, although no longer rotating, does not fracture as quickly as the smaller arm; this may be because the amount of fracturing depends on the speed of layer rotation.
(10) The optical switching time (~5 s) is longer than the time for one set of layers to disrupt (~2 s), but comparable to the time for the other set of layers to disrupt (~6 s).

This is the first time that layer motion has been directly observed during the electric field induced switching of smectic A phase devices. The experimental geometry did not allow confirmation that the final switched state was layered, although it is believed that a layer structure would have (re)appeared once the molecules had stopped rotating. It would be interesting to confirm this in a subsequent experiment.

Thanks are due to Dr M. Wiltshire for useful discussions and to Dr C. Carboni for help with experiments. Financial support form the Engineering and Physical Science Research Council, General Electric Company, Daresbury Laboratory, and Leverhulme Foundation is gratefully acknowledged.

References

[1] Rieker, T. R., and Clark, N. A., 1988, *Phys. Rev. A*, **37,** 1053.
[2] Goodby, J. W., 1991, *Ferroelectric Liquid Crystals. Principles, Properties and Applications*, (*Ferroelectricity and Related Phenomena,* Vol. 7) (UK: Gordon and Breach Science Publishers).
[3] Takanishi, Y., Ouchi, Y., Takezoe, H., and Fukuda, A., 1989, *Jpn J. appl. Phys.*, **28,** L487.
[4] Ouchi, Y., Takanishi, Y., Takezoe, H., and Fukuda, A., 1989, *Jpn. J. appl. Phys.*, **28,** 2547.
[5] Taylor, L., Richardson, R. M., Ebbutt, J., and Jones, J. C., 1995, *Mol. Cryst. liq. Cryst.*, **263,** 255.
[6] Morse, S. A., and Gleeson, H. F., *Liq. Cryst.*, in press.
[7] Blinov, L. M., and Chigrinov, V. G., 1994, *Electrooptic Effects in Liquid Crystal Materials* (Springer).
[8] Goscianski, M., Leger, L., and Mircea-Roussel, A., 1975, *J. de Phys. Lett*, **36,** L313.

[9] HARENG, M., LE BERRE, S., and METZGER, J. J., 1975, *Appl. Phys. Lett.*, **27,** 575.
[10] ROUT, D. K., and CHOUDHARY, R. N. P., 1989, *Mol. Cryst. liq. Cryst.*, **166,** 75.
[11] JÁKLI, A., and SAUPE, A., 1992, *Mol. Cryst. liq. Cryst.*, **222,** 101.
[12] GLEESON, H. F., and MORSE, A., 1996, *Liq. Cryst.*, **21,** 755.
[13] GLEESON, H. F., CARBONI, C., and MORSE, A., 1995, *Rev. sci. Instrum.*, **66,** 3563.
[14] RIEKER, T. P., CLARK, N. A., SMITH, G. S. and SAFINYA, C. R., 1989, *Liquid Crystals*, **6** (5), 565.